Opt Quant Electron (2007) 39:361–375
DOI 10.1007/s11082-007-9102-8

Quasi phase matching in two-dimensional nonlinear photonic crystals

Ady Arie · Nili Habshoosh · Alon Bahabad

Received: 9 July 2006 / Accepted: 12 December 2007 / Published online: 16 June 2007

Abstract We analyze quasi-phase-matched (QPM) conversion efficiency of the five possible types of periodic two-dimensional nonlinear structures: Hexagonal, square, rectangular, centered-rectangular, and oblique. The frequency conversion efficiency, as a function of the two-dimensional quasi-phase-matching order, is determined for the general case. Furthermore, it is demonstrated for two basic feasible motifs, a circular motif and a rectangular motif. This enables to determine the optimal motif dimensions for achieving the highest conversion efficiency. We find that a rectangular motif is more efficient than a circular motif for quasi-phase-matched processes that rely on a single reciprocal lattice vector (RLV), and that under optimal choice of motif dimensions, it converges into a one-dimensional periodic structure. In addition, in a few specific cases we found that higher order QPM can be significantly more efficient than lower order QPM.

Keywords Quasi phase matching · Nonlinear photonic crystals · Nonlinear frequency conversion · Second harmonic generation

1 Introduction

In recent years, since the introduction of two-dimensional nonlinear photonic crystals (2D NLPC) by Berger (1998), there has been a growing interest in these structures and in their potential applications. They were studied for non-collinear second harmonic generation (SHG) (Broderick et al. 2000), for simultaneous wavelength interchange (Chowdhury et al. 2001), for third and fourth harmonic generation (Broderick et al. 2002; Saltiel and Kivshar 2000), and proposed for realization of all optical effects, e.g., all optical deflection and splitting (Saltiel and Kivshar 2002). Various methods have been tested for fabrication of 2D NLPC, including electric field poling (Broderick et al. 2000; Chowdhury et al. 2001

A. Arie (✉) · N. Habshoosh · A. Bahabad
Department of Physical Electronics, School of Electrical Engineering, Tel-Aviv University, Tel-Aviv 69978, Israel
e-mail: ady@eng.tau.ac.il

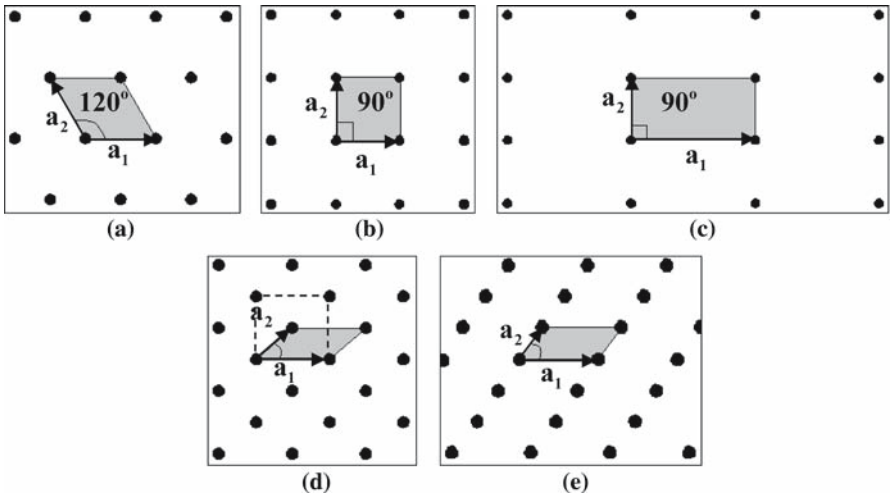

Fig. 1 The five different types of Bravais lattices: (**a**) Hexagonal, (**b**) Square, (**c**) Rectangular, (**d**) Centered-rectangular, where the dashed lines form a rectangle, (**e**) Oblique

Ni et al. 2003; Peng et al. 2003) and electron beam irradiation (Glickman et al. 2006) of $LiNbO_3$. Recently, two-dimensional nonlinear structures with quasi-periodic modulation have been analyzed (Lifshitz et al. 2005) and experimentally demonstrated (Bratfalean et al. 2005).

As is well known from solid-state physics (Kittel 1995), 2D periodic structures can be classified by five Bravais lattices: Hexagonal, square, rectangular, centered-rectangular, and oblique, as can be seen in Fig. 1. In order to convert a lattice into a 2D NLPC, we convolve each one of the lattice points with a nonlinear motif—i.e., some geometrical shape in which the nonlinear coefficient sign is different from the background sign. For example, in ferroelectric crystals, e.g., $LiNbO_3$ and $LiTaO_3$, the sign of the nonlinear coefficient can be locally inverted by a domain reversal. In the first experimental demonstration of 2D NLPC by Broderick et al. (2000), hexagonal lattice was used in $LiNBO_3$, and the motif was also hexagonal. Usually, in other materials, like glasses (Myers et al. 1991), only the motif is poled thus having a non-zero nonlinear coefficient, whereas the remaining background is un-poled and therefore has a zero nonlinear coefficient.

In order to optimally design and use a 2D NLPC, one needs to know the conversion efficiency for any given lattice, its dependence on the shape and size of the motif, and its dependence on the quasi phase matching (QPM) orders. Although part of the cases have been discussed in previous works (Berger 1998; Wang and Gu 2001), as far as we know there is no systematic study on the efficiency dependence of all the structure parameters. In this work, we study the conversion efficiency of structures made of the five different Bravais lattices and explicitly analyze for two basic feasible motifs, a circular motif and a rectangular motif. We also determine the optimal dimensions of these motifs for some QPM processes in each lattice.

The conversion efficiency for two of the five possible lattices (hexagonal and square), for the case of a circular motif was previously studied by Wang and Gu (2001), with identical results for the present analysis of square lattice, but some differences appear for the case of hexagonal lattice. In addition they also analyze a triangular structure. We note that in the photonic crystals community, a "triangular" lattice is what we refer to as hexagonal lattice,

while "hexagonal" or "honey-comb" lattice is a hexagonal lattice with a missing point in the middle of each hexagon. This "honey-comb" lattice can be analyzed using the tools presented in this paper, e.g., it can be written as the difference between one hexagonal lattice with a base vector of length a, and a second hexagonal lattice with a base vector of length $\sqrt{3}a$. Our results for the hexagonal lattice are different than those of Wang and Gu (2001) for the "triangular" as well as the "hexagonal" lattices.

As far as we know, 2D QPM conversion efficiency of rectangular, centered-rectangular, and oblique structures have not been published before. In addition, previous publications (Berger 1998; Wang and Gu 2001) concentrated on circular motifs. Results concerning rectangular motif have not been published previously.

A general analysis of quasi-phase-matched interactions in 2D NLPC is given in Sect. 2. This includes a mathematical description of the real and reciprocal lattice, and analysis of the effect of the lattice, motif and interaction area on the generated electric field and intensity. In Sect. 3, the normalized conversion efficiency of the five 2D Bravais lattices with circular and rectangular motifs is described, followed by a specific study of these motif optimum dimensions for some specific QPM orders. The results are discussed and summarized in Sect. 4.

2 General analysis of a periodic two-dimensional nonlinear photonic crystal

2.1 The real lattice

A two-dimensional nonlinear lattice is defined by two primitive, non-parallel vectors $\mathbf{a_1}$, $\mathbf{a_2}$, so that each lattice point is given by

$$\mathbf{r}_{mn} = m\mathbf{a_1} + n\mathbf{a_2} \tag{1}$$

The lattice is represented by a set of distributed Dirac delta functions:

$$u(\mathbf{r}) = \sum_{m,n} \delta(\mathbf{r} - \mathbf{r}_{mn}) = \sum_{m,n} \delta(\mathbf{r} - m\mathbf{a_1} - n\mathbf{a_2}) \tag{2}$$

The lattice can be converted into a nonlinear photonic crystal by convolving the lattice points with a suitable nonlinear optical motif. For example, we can have a circular pattern, defining a positive value for the nonlinear coefficient, centered at each one of the lattice points. These motifs are surrounded by a background with a different nonlinear coefficient. The pattern outside the circular motifs, may be linear (zero nonlinearity, as for example is the case for patterns made of poled and un-poled glass), or may have an opposite sign of the nonlinear coefficient (as is the case in domain inverted ferroelectric crystals). For the case of circular motif, the motif function $s(\mathbf{r})$ is given by

$$s(\mathbf{r}) = \mathrm{circ}\left(\frac{r}{R}\right) \equiv \begin{cases} 1 & r < R \\ 0 & \text{elsewhere} \end{cases} \tag{3}$$

where $r = |\mathbf{r}|$.

Another possibility is a rectangular motif, defined as:

$$s(\mathbf{r}) = s(x, y) = \mathrm{rect}\left(\frac{x}{X}\right) \cdot \mathrm{rect}\left(\frac{y}{Y}\right) \tag{4}$$

where the rect function is defined by:

$$\mathrm{rect}(x) = \begin{cases} 1 & |x| < 1/2 \\ 0 & \text{elsewhere} \end{cases} \tag{5}$$

If the background is nonlinear (with opposite sign to the motif nonlinear coefficient) the motif function has values of 1 and (−1) instead of 1 and 0. This amount in a DC shift in the Fourier transform of the overall structure function (the result, as implied through Sect. 2.3, is doubling of the electric field conversion efficiency for a QPM process). To simplify the following analysis we shall assume first that the background has a zero nonlinear coefficient, and later (in Sect. 3) adjust the final results in order to account for non-zero background.

The lattice area is restricted by the crystal physical size and by an effective interaction area. Let us denote the area function as $a(\mathbf{r})$. Let us assume that the area function is rectangular with a length L and width W. In that case, the area function is:

$$a(\mathbf{r}) = a\,(x,\, y) = \mathrm{rect}\left(\frac{x}{L}\right) \cdot \mathrm{rect}\left(\frac{y}{W}\right) \tag{6}$$

The relevant Cartesian component of the nonlinear dielectric tensor as a function of position in a nonlinear photonic crystal can be therefore expressed mathematically as

$$\chi_{ij}^{(2)}\,(\mathbf{r}) = 2d_{ij} \times g(\mathbf{r}) = 2d_{ij} \times a(\mathbf{r}) \times [u(\mathbf{r}) \otimes s(\mathbf{r})] \tag{7}$$

where d_{ij} is the value of the nonlinear susceptibility tensor for the Cartesian indices i and j, and $\otimes$ is the convolution operator. $g(\mathbf{r})$ is a normalized and dimensionless function that represents the space dependence of the nonlinear coefficient function.

2.2 The reciprocal lattice

Similar to the analysis of crystals in solid-state physics (Kittel 1995), it is useful to define a reciprocal lattice for $u(\mathbf{r})$ using two primitive vectors that together with the direct lattice primitive vectors obey the following orthogonality relation:

$$\mathbf{a_i} \cdot \mathbf{b_j} = 2\pi\delta_{\mathbf{ij}} \tag{8}$$

The reciprocal lattice points are given by

$$\mathbf{K}_{mn} = m\mathbf{b_1} + n\mathbf{b_2} \tag{9}$$

The reciprocal lattice function is the two-dimensional Fourier transform of the direct (or "real") lattice function:

$$\begin{aligned} U\,(\mathbf{f}) &= \frac{1}{A_{UC}} \sum_{m,n} \delta\left(\mathbf{f} - \frac{m\mathbf{b_1}}{2\pi} - \frac{n\mathbf{b_2}}{2\pi}\right) = \frac{(2\pi)^2}{A_{UC}} \sum_{m,n} \delta\,(\mathbf{K} - m\mathbf{b_1} - n\mathbf{b_2}) \\ &= \frac{(2\pi)^2}{A_{UC}} \sum_{m,n} \delta\,(\mathbf{K} - \mathbf{K}_{mn}) \end{aligned} \tag{10}$$

Here $A_{UC} = \left|a_{1x}a_{2y} - a_{1y}a_{2x}\right|$ is the area of the unit cell (Giacovazzo et al. 2002), $\mathbf{f}$ is the spatial frequency in the two-dimensional Fourier space, $\mathbf{K} = 2\pi\mathbf{f}$ and $\mathbf{a_1} = \left(a_{1x}, a_{1y}\right)$, $\mathbf{a_2} = \left(a_{2x}, a_{2y}\right)$.

For the following discussion, it is also useful to calculate the Fourier transform of $g(\mathbf{r})$:

$$G(\mathbf{f}) = \mathrm{FT}\,\{g(\mathbf{r})\} = U(\mathbf{f}) \otimes A(\mathbf{f}) \times S(\mathbf{f}) \tag{11}$$

Where $A(\mathbf{f})$ and $S(\mathbf{f})$ are the Fourier transform functions of the area function and motif function, respectively.

For some specific motif functions, $S(\mathbf{f})$ is known analytically. For example, in the case of circular motif of radius R, the Fourier transform is:

$$S(\mathbf{f}) = \frac{R}{\mathrm{f}} J_1(2\pi R\mathrm{f}), \quad \mathrm{f} = |\mathbf{f}| = \left(f_x^2 + f_y^2\right)^{1/2} \tag{12}$$

And for a rectangular motif:

$$S(\mathbf{f}) = S\left(f_x, f_y\right) = XY \operatorname{sinc}(f_x X) \operatorname{sinc}\left(f_y Y\right) \tag{13}$$

where the sinc function is defined as $\operatorname{sinc}(x) \equiv \sin(\pi x)/(\pi x)$.

Similarly, the Fourier transform of a rectangular area function of dimensions $L \times W$ is:

$$A(\mathbf{f}) = A\left(f_x, f_y\right) = LW \operatorname{sinc}(f_x L) \operatorname{sinc}\left(f_y W\right) \tag{14}$$

For the case of infinite area, (L, W much larger than the unit cell dimensions), the space-dependent part of the nonlinear susceptibility can be expressed as the following sum:

$$g(\mathbf{r}) = \sum_{m,n} G_{mn} \exp(-i\mathbf{K}_{mn} \cdot \mathbf{r}) \tag{15}$$

This equation shows clearly the relation between the reciprocal lattice vectors (RLV) and the nonlinear susceptibility as a function of space.

In this case the Fourier coefficient becomes

$$G_{mn} = \frac{1}{A_{UC}} S(\mathbf{K}_{mn}/2\pi) \tag{16}$$

As will be shown in the next section, the conversion efficiency in a 2D NLPC is proportional to $|G_{mn}|^2$. Equation 16 shows the combined effect of the lattice (through the unit cell area), the motif (through its Fourier transform function S) and the QPM orders m, n on the nonlinear process.

2.3 Wave equations in 2D NLPC

We consider now the case of second harmonic generation in a 2D NLPC. The results shown here can be easily generalized to other second-order nonlinear processes, e.g., sum frequency generation and difference frequency generation. We assume that a plane wave at the frequency ω propagates in the transverse plane of a 2D NLPC. This wave generates a second harmonic wave owing to the second order susceptibility of the material. We assume that the fundamental frequency is linearly polarized along one of the 2D NLPC axes, and we concentrate only in a specific linear polarization of the generated second harmonic wave. The coupling between the two beams is given by the appropriate element of the nonlinear susceptibility tensor d_{ij}.

Let us write the relevant component of the second harmonic wave as

$$\tilde{E}_{2\omega}(\mathbf{r}, t) = \frac{1}{2} E_{2\omega}(\mathbf{r}) \exp[i(2\omega t - \mathbf{k}_{2\omega} \cdot \mathbf{r})] + \text{c.c.} \tag{17}$$

We assume that the nonlinear conversion efficiency is low, hence the pump amplitude can be assumed constant throughout the entire interaction length (non-depletion approximation). We further assume that the slowly varying envelope approximation applies for the second harmonic wave. Under these assumptions it can be shown that:

$$\mathbf{k}_{2\omega} \cdot \nabla E_{2\omega}(\mathbf{r}) = -i \frac{\omega^2}{c^2} E_\omega^2 \chi_{ij}^{(2)}(\mathbf{r}) \exp[i(\mathbf{k}_{2\omega} - 2\mathbf{k}_\omega) \cdot \mathbf{r}] \tag{18}$$

If the 2D NLPC is large enough we can use Eq. 15 for the second order susceptibility, and so:

$$\mathbf{k}_{2\omega} \cdot \nabla E_{2\omega}(\mathbf{r}) = -2i\frac{\omega^2}{c^2} E_\omega^2 d_{ij} \sum_{mn} G_{mn} \exp\left[i\left(\mathbf{k}_{2\omega} - 2\mathbf{k}_\omega - \mathbf{K}_{mn}\right) \cdot \mathbf{r}\right] \tag{19}$$

Significant build-up of the second harmonic wave requires phase matching, i.e.,

$$\mathbf{k}_{2\omega} - 2\mathbf{k}_\omega - \mathbf{K}_{mn} \approx 0.$$

This phase-matching condition is just a crystal-momentum conservation law: the required momentum balance for the interaction is accomplished through a RLV. Usually we can assume that if the phase matching condition is achieved by some order (m, n), it would be the only order which contributes to the build-up of the second harmonic while all the other orders contributes negligible oscillating terms.

This process can also be analyzed in Fourier space by integrating Eq. 18 above over a rectangular area of width W and length L (see an example (Russel et al. 2001)). The result is the second harmonic amplitude after an interaction length of L:

$$E_{2\omega}(\Delta\mathbf{k}) = \frac{-2i\omega^2 E_\omega^2 d_{ij}}{k_{2\omega} c^2 W} \iint_A g(\mathbf{r}) \exp\left(-i\Delta\mathbf{k} \cdot \mathbf{r}\right) \mathrm{d}a \tag{20}$$

where $\Delta\mathbf{k} = \mathbf{k}_{2\omega} - 2\mathbf{k}_\omega$ is the phase-mismatch vector. If the integration area is given through the function $a(\mathbf{r})$ defined in Sect. 2.1, we can use $g(\mathbf{r}) = a(\mathbf{r}) \times (u(\mathbf{r}) \otimes s(\mathbf{r}))$ and set the integration limits to infinity and so:

$$E_{2\omega}(\Delta\mathbf{k}) = \frac{\kappa}{W} G(\Delta\mathbf{k}) \tag{21}$$

where $G(\Delta\mathbf{k})$ is just the two-dimensional Fourier transform of $g(\mathbf{r})$ and κ is a constant defined as:

$$\kappa = \frac{-2i\omega^2 E_\omega^2 d_{ij}}{k_{2\omega} c^2} = \frac{-i\omega E_\omega^2 d_{ij}}{n_{2\omega} c} \tag{22}$$

From Eq. 21 we can see that the field amplitude evaluation for some specific phase mismatch value $\Delta\mathbf{k} = \Delta\mathbf{k_0}$ is proportional to $|G(\Delta\mathbf{k_0})|$.

If phase matching condition is achieved by some order (m, n) then the integral above is dominated by this order and we can write:

$$\begin{aligned} E_{2\omega}(\Delta\mathbf{k} \approx \mathbf{K}_{mn}) \cong \kappa L G_{mn} \exp\left[-i\left(\frac{\Delta k_{mn,x} L}{2} + \frac{\Delta k_{mn,y} W}{2}\right)\right] \\ \times \mathrm{sinc}\left(\frac{\Delta k_{mn,x} L}{2\pi}\right) \mathrm{sinc}\left(\frac{\Delta k_{mn,y} W}{2\pi}\right) \end{aligned} \tag{23}$$

where $\Delta\mathbf{k}_{mn} = \Delta\mathbf{k} - \mathbf{K}_{mn} = \Delta k_{mn,x}\hat{x} + \Delta k_{mn,y}\hat{y}$.

For perfect quasi-phase-matching $\Delta k_{mn,x} = \Delta k_{mn,y} = 0$ and so:

$$E_{2\omega}(\Delta\mathbf{k} = \mathbf{K}_{mn}) \cong \kappa L G_{mn} \tag{24}$$

The fundamental and second harmonic amplitudes are related to the corresponding intensities by:

$$I_\omega = \frac{1}{2} n_\omega \sqrt{\frac{\varepsilon_0}{\mu_0}} |E_\omega|^2, \quad I_{2\omega} = \frac{1}{2} n_{2\omega} \sqrt{\frac{\varepsilon_0}{\mu_0}} |E_{2\omega}|^2 \tag{25}$$

Hence, the intensity of the second harmonic for the case of perfect quasi-phase-matching after an interaction length L is:

$$I_{2\omega}(L) = \frac{2\omega^2 d_{ij}^2 |G_{mn}|^2}{n_{2\omega} n_\omega^2 c^3 \varepsilon_0} I_\omega^2 L^2 \tag{26}$$

and so the interaction efficiency is proportional to the absolute square of the relevant Fourier coefficient$|G_{mn}|^2$. We shall now relate to $|G_{mn}|^2$ as the normalized efficiency.

3 Conversion efficiency for specific types of 2D periodic structures

3.1 General expressions for Fourier coefficients

Without loss of generality, we can define the coordinate system so that one of its axes is in the same direction as that of the $\mathbf{a_1}$ primitive vector. Denoting the angle between the two primitive vectors as γ, the primitive vectors of the real and reciprocal lattice are:

$$\begin{aligned} &\mathbf{a_1} = (a_1, 0), \quad \mathbf{a_2} = (a_2 \cos\gamma, a_2 \sin\gamma) \\ &\mathbf{b_1} = \frac{2\pi}{a_1}\left(1, -\frac{1}{\tan\gamma}\right), \quad \mathbf{b_2} = \frac{2\pi}{a_2}\left(0, \frac{1}{\sin\gamma}\right) \end{aligned} \tag{27}$$

We shall now analyze the conversion efficiency of the five possible 2D lattices. For each one of them we present in Table 1 the primitive vectors, RLVs and the unit cell areas.

As was shown in the previous section, the nonlinear conversion efficiency depends on the Fourier coefficient G_{mn} of the normalized nonlinear susceptibility. These Fourier coefficients are presented in Table 2a and b for each one of the lattice types for two different motifs, circular, and rectangular, respectively. These two motifs were chosen since they represent two basic cases of two-dimensional modulation of the nonlinear coefficient. The circular motif is suitable for materials that are nearly isotropic in the X–Y plane. Nearly circular motifs have been demonstrated experimentally in two-dimensionally poled $LiNbO_3$ (Ni et al. 2003; Glickman et al. 2006). On the other hand, a rectangular motif is suitable

Table 1 Primitive vectors, RLVs, and unit cell area for the five lattice types

Lattice types	Primitive vectors	RLVs	Unit cell area
Hexagonal $\gamma = 120°$	$\mathbf{a_1} = (a, 0)$ $\mathbf{a_2} = a\left(-\frac{1}{2}, \frac{\sqrt{3}}{2}\right)$	$\mathbf{b_1} = \frac{2\pi}{a}\left(1, \frac{1}{\sqrt{3}}\right)$ $\mathbf{b_2} = \frac{4\pi}{a\sqrt{3}}(0, 1)$	$A_{UC} = \frac{a^2\sqrt{3}}{2}$
Square $\gamma = 90°$	$\mathbf{a_1} = (a, 0)$ $\mathbf{a_2} = (0, a)$	$\mathbf{b_1} = \frac{2\pi}{a}(1, 0)$ $\mathbf{b_2} = \frac{2\pi}{a}(0, 1)$	$A_{UC} = a^2$
Rectangular $\gamma = 90°$	$\mathbf{a_1} = (a_1, 0)$ $\mathbf{a_2} = (0, a_2)$	$\mathbf{b_1} = \frac{2\pi}{a_1}(1, 0)$ $\mathbf{b_2} = \frac{2\pi}{a_2}(0, 1)$	$A_{UC} = a_1 a_2$
Centered-rectangular $\gamma \in [0°, 90°]$	$\mathbf{a_1} = (a, 0)$ $\mathbf{a_2} = a\left(\frac{1}{2}, \frac{1}{2}\tan\gamma\right)$	$\mathbf{b_1} = \frac{2\pi}{a}\left(1, \frac{-1}{\tan\gamma}\right)$ $\mathbf{b_2} = \frac{4\pi}{a}\left(0, \frac{1}{\tan\gamma}\right)$	$A_{UC} = \frac{a^2}{2}\tan\gamma$
Oblique $\gamma \in [0°, 180°]$	$\mathbf{a_1} = (a_1, 0)$ $\mathbf{a_2} = a_2(\cos\gamma, \sin\gamma)$	$\mathbf{b_1} = \frac{2\pi}{a_1}\left(1, \frac{-1}{\tan\gamma}\right)$ $\mathbf{b_2} = \frac{2\pi}{a_2}\left(0, \frac{1}{\sin\gamma}\right)$	$A_{UC} = a_1 a_2 \sin\gamma$

Table 2 Fourier coefficient of a (a) circular motif and (b) rectangular motif

Lattice types	Fourier coefficients
(a) Fourier coefficient of a circular motif	
Hexagonal	$G_{mn} = \frac{2R}{a\sqrt{m^2+n^2+mn}} J_1\left(\frac{4\pi R}{a\sqrt{3}}\sqrt{m^2+n^2+mn}\right)$
Square	$G_{mn} = \frac{2R}{a\sqrt{m^2+n^2}} J_1\left(\frac{2\pi}{a} R\sqrt{m^2+n^2}\right)$
Rectangular	$G_{mn} = \frac{2R}{\sqrt{(ma_2)^2+(na_1)^2}} J_1\left[2\pi R\sqrt{\left(\frac{m}{a_1}\right)^2+\left(\frac{n}{a_2}\right)^2}\right]$
Centered-rectangular	$G_{mn} = \frac{2R\cdot 2\cos\gamma}{a\sqrt{m^2+4n^2\cos^2\gamma-4mn\cos^2\gamma}} J_1\left(\frac{2\pi R}{a\sin\gamma}\sqrt{m^2+4n^2\cos^2\gamma-4mn\cos^2\gamma}\right)$
Oblique	$G_{mn}=\frac{2R}{\sqrt{a_1a_2}\sqrt{\frac{m^2a_2}{a_1}+\frac{n^2a_1}{a_2}-2mn\cos\gamma}} J_1\left(\frac{2\pi R}{\sin\gamma\sqrt{a_1a_2}}\sqrt{\frac{m^2a_2}{a_1}+\frac{n^2a_1}{a_2}-2mn\cos\gamma}\right)$
(b) Fourier coefficient of a rectangular motif	
Hexagonal	$G_{mn} = \frac{4XY}{a^2\sqrt{3}}\operatorname{sinc}\left(m\frac{X}{a}\right)\operatorname{sinc}\left[\frac{Y}{a\sqrt{3}}(m+2n)\right]$
Square	$G_{mn} = \frac{2XY}{a^2}\operatorname{sinc}\left(m\frac{X}{a}\right)\operatorname{sinc}\left(n\frac{Y}{a}\right)$
Rectangular	$G_{mn} = \frac{2XY}{a_1a_2}\operatorname{sinc}\left(m\frac{X}{a_1}\right)\operatorname{sinc}\left(n\frac{Y}{a_2}\right)$
Centered-rectangular	$G_{mn} = \frac{4XY}{a^2\tan\gamma}\operatorname{sinc}\left(m\frac{X}{a}\right)\operatorname{sinc}\left[\frac{Y}{a\tan\gamma}(-m+2n)\right]$
Oblique	$G_{mn} = \frac{2XY}{a_1a_2\sin\gamma}\operatorname{sinc}\left(m\frac{X}{a_1}\right)\operatorname{sinc}\left[\frac{Y}{\sin\gamma}\left(\frac{-m\cos\gamma}{a_1}+\frac{n}{a_2}\right)\right]$

for strongly an-isotropic materials. For example, electric-field poling of $KTiOPO_4$ usually results in lines parallel to the Y axis, hence a rectangular motif is the suitable choice for two-dimensional modulation of the nonlinear coefficient (Jankovic et al. 2003). A numerical optimization procedure for general shapes of motifs was given by Norton and de-Sterke (2003), however its experimental implementation requires to modulate the nonlinear coefficient with high spatial resolution.

According to Eq. 12, the Fourier transform of a circular motif with a radius R, depends on a 1st order Bessel function. In Table 2a we present the Fourier coefficients for all five lattice types with a circular motif as function of R, the primitive vectors magnitude and the QPM orders (m, n).

The Fourier transform of a rectangular motif with length X and width Y, acts as a two-dimensional sinc function, see Eq. 13. Note that under the selection of primitive vectors (Eq. 27), one of the rectangular motif's edges is parallel to $\mathbf{a_1}$. The Fourier coefficient for a lattice with a rectangular motif is a function of the motif dimensions (X, Y), the primitive vectors magnitude and the relevant QPM order (m, n). Table 2b displays it for all five lattice types.

Note that the Fourier coefficients in Table 2a and b are suitable for the case in which the background has an opposite nonlinear coefficient with respect to the motif. This is the case for domain-inverted ferroelectrics. If the background has zero-nonlinearity, the Fourier coefficients in the two tables should be multiplied by 1/2.

3.2 Efficiency for specific QPM orders

We shall now examine in more detail the efficiency as a function of the ratio between the motif size and the primitive vectors magnitude, for specific QPM orders. This enables to determine

the highest possible efficiency for a given structure and the required dimensions and shape of the motif. Furthermore, it allows determining motif shapes that will completely null the nonlinear conversion efficiency (which, for example, can be useful to nullify unwanted processes). We concentrate on three out of the five lattice types, namely the hexagonal, square, and rectangular lattices. For the other two lattices (centered-rectangular and oblique), the motif dimension and the efficiency will depend on the angle γ between the two primitive vectors.

We chose two specific QPM orders: $(m, n) = (1, 0)$ and $(m, n) = (1, 1)$. The first one is usually the most efficient process in a 2D nonlinear structure, however it relies on only one of the two primitive vectors. The second order is usually the most efficient process that relies on both primitive vectors although, as shown below, in some cases one may get higher efficiency with a different choice of (m, n) order.

In Sect. 3.2.1 we examine the normalized efficiency as a function of the ratio between the circle radius and a primitive vector length in the case of a circular motif. In Sect. 3.2.2 we study the normalized efficiency as a function of the ratio between one of the rectangle dimensions and the length of a primitive vector in the case of a rectangular motif.

3.2.1 Circular motif

In the following analysis, we shall limit the motif size, in order to avoid overlap between motifs of adjacent lattice points. For each lattice, this sets the maximum allowed motif size.

For a hexagonal lattice, due to the fact that the two primitive vectors have the same magnitude and an angle of 120° between them, the radius of the circular motif has possible values from zero to half the primitive vector magnitude a. Figure 2 displays the normalized efficiency of a hexagonal lattice with a circular motif for the two QPM orders mentioned before, as a function of the R/a ratio. In the drawings of 2D NLPCs in Figs. 2–7, the gray areas represent a certain sign of the nonlinear coefficient, whereas the white areas represent the opposite sign. As can be seen, the order $(m = 1, n = 0)$ is more efficient, as expected, and the maximum efficiency (0.118) is achieved when $R/a = 0.331$. For $(m = 1, n = 1)$, the maximum efficiency is 0.03 when $R/a = 0.439$. Also note that for $R/a = 0.305$ the efficiency of the (1, 1) QPM order drops to zero.

In the case of square lattice, the radius of the circular motif has possible values from zero to half the primitive vector magnitude a in order to prevent overlapping. This is the same

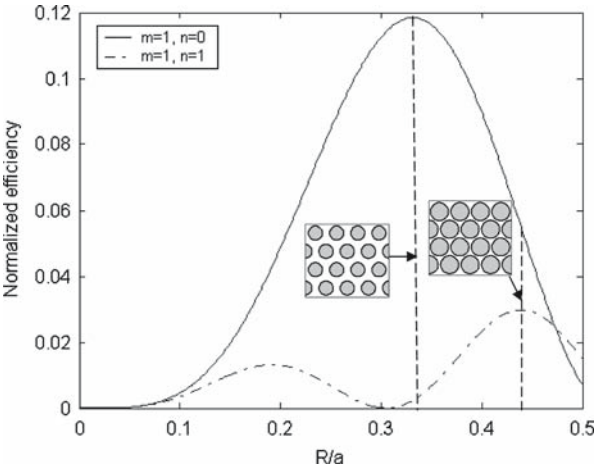

Fig. 2 Normalized efficiency for a hexagonal lattice with circular motif as a function of the motif radius to primitive vector magnitude ratio. Solid and dash-dot lines represent the efficiency curves for QPM orders (1, 0) and (1, 1), respectively. The insets show the shape of the 2D NLPC for R/a ratios that maximize the (1, 0) and (1, 1) QPM processes

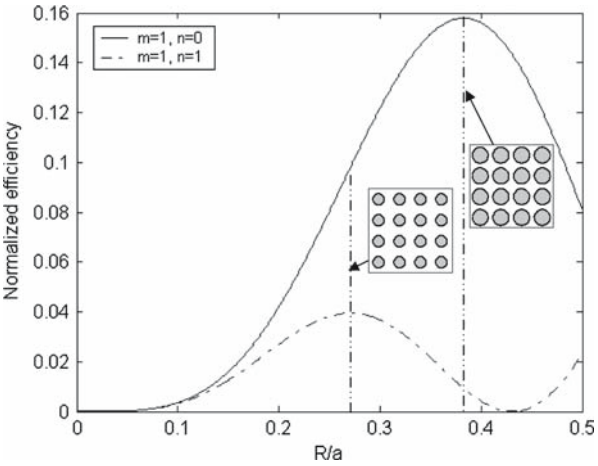

Fig. 3 Normalized efficiency for a square lattice with circular motif as a function of the motif radius to primitive vector magnitude ratio. Solid and dash-dot lines represent the efficiency curves for QPM orders (1, 0) and (1, 1) respectively. The insets show the shape of the 2D NLPC for R/a ratios that maximize the (1, 0) and (1, 1) QPM processes

range as in the first case of a hexagonal lattice. The normalized efficiency of the (1, 0) and (1, 1) orders as a function of the normalized motif radius is shown in Fig. 3.

The maximum efficiency of the (1, 0) order is 0.158 when $R/a = 0.383$, and for the (1, 1) order the maximum efficiency is 0.04 when $R/a = 0.271$. Note that in both cases, the square lattice is more efficient than the hexagonal lattice. Also note that the efficiency of the (1, 1) order is zero for $R/a = 0.431$.

For a rectangular lattice, and for the (1, 0) QPM order, the Fourier coefficient is composed of two independent functions:

$$G_{10} = \frac{2R}{a_2} \cdot J_1\left(\frac{2\pi R}{a_1}\right) \tag{28}$$

The left expression on the right hand side depends only on R/a_2, whereas the right expression is a Bessel function which depends only on R/a_1. The maximum value of G_{10} is equal to the multiplication between the maximum of each one of the functions. It is easy to see that the maximum of the first function is achieved when R/a_2 is set to the maximum value of 0.5. In this case, the motifs of adjacent lattice points along the $\mathbf{a_2}$ direction are just touching each other. Figure 4 shows the normalized efficiency $|G_{10}|^2$ as function of R/a_1, when $R/a_2 = 0.5$. Note that in this case, the rectangular lattice is the most efficient structure, and provides significantly higher efficiency with respect to the hexagonal and rectangular lattice. Also note that the shape of the optimal lattice (for phase matching a single process), see inset of Fig. 4, is similar to that of a one-dimensional periodic structure. As will be shown below, if a rectangular motif is used instead of a circular motif, the optimal lattice shape becomes identical to a one-dimensional structure.

For the (1, 1) order, the maximum efficiency is similar to the case of a square lattice ($|G_{11}|^2 = 0.04$ when $R/a_1 = R/a_2 = 0.271$).

3.2.2 Rectangular motif

In order to prevent overlapping of rectangular motifs of adjacent lattice points, the possible ratios between the motif dimensions and the primitive vectors are:

$$0 < X < a_1; \quad 0 < Y < a_2 \sin\gamma \tag{29}$$

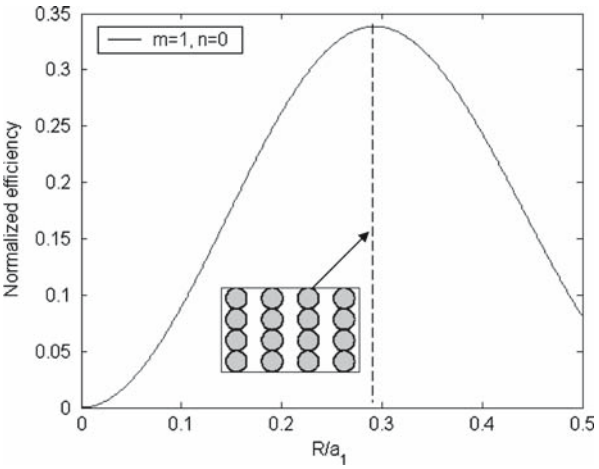

Fig. 4 Normalized efficiency for a rectangular lattice with circular motif for m=1, n=0, R/a_2=0.5 as a function of the motif radius to primitive vector magnitude ratio. The inset shows the 2D NLPC for a specific R/a_1 ratio that maximizes the efficiency

In case of a hexagonal lattice, the Fourier coefficient is composed of two independent sinc functions, see Table 2b. Hence, the maximum Fourier coefficient is equal to the multiplication between the maximum of each one of the independent functions.

For the (1, 0) QPM order the maximum value of $|G_{10}|^2$ is equal to 0.164 and it is achieved when $X = 0.5a$ and $Y = a\sqrt{3}/2 = a \sin 120°$, the structure has the shape of a chess-board. Note that this is ∼39% times more efficient than the Fourier coefficient in the case of a circular motif, where $|G_{10}|^2$ is 0.118.

For the (1, 1) QPM order, the maximum value of $|G_{11}|^2$ is equal to 0.018 and it is achieved when $X = 0.5a$ and $Y = a/2\sqrt{3} = a \sin 120°/3$. Unlike the (1, 0) order, this is less efficient than the circular motif, where $|G_{11}|^2 = 0.0298$. The (1, 1) QPM order has another maximum with the same efficiency when $X = 0.5a, Y = a\sqrt{3}/2 = a \sin 120°$, which is also the optimal choice for the (1, 0) order. In addition, the efficiency of the (1, 1) QPM order becomes zero when $X = 0.5a$ and $Y = 0.578a = a \sin 120° \times 0.667$.

An interesting phenomenon occurs for the (2, −1) QPM order. Usually, the efficiency is inversely proportional to the square of the QPM order indices m and n, hence we expect that as (m, n) becomes higher, the maximum normalized efficiency will drop. However, as seen in Fig. 5, the maximum value $\left|G_{2(-1)}\right|^2 = 0.1013$ is considerably higher than the maximum value of $|G_{11}|^2$. This effect can be understood by examining the normalized efficiency expression in Table 2b. The Fourier coefficient is a product of two sinc functions, one that depends on mX/a and the other that depends on $(m + 2n)Y \Big/ \left(a\sqrt{3}\right)$. Hence, for the (2, −1) order, the argument of the second sinc function becomes zero, and the maximum unity value is obtained. This can be explained by noticing that the reciprocal lattice vector $\mathbf{K}_{2(-1)}$ is shorter than the $\mathbf{K}_{11}$ vector. In fact, for any (m, n) values that satisfy $m + 2n = 0$ the QPM process will be more efficient than neighboring orders in which this condition is not satisfied. Conditions for efficient QPM orders with high (m, n) values can also be derived in the case of centered-rectangular and oblique lattices, for the circular motif and rectangular motif using Table 2a and b, respectively.

The highest efficiency of a hexagonal lattice, with our specific choice of rectangular motif is obtained for the (0, 1) order. In this case, by selecting $X = a$ and $Y = a\sqrt{3}/4$ the rectangular motifs merge into a continuous line in the X direction as can be seen in Fig. 6a, and we obtain exactly a one-dimensional periodic structure, with a normalized efficiency

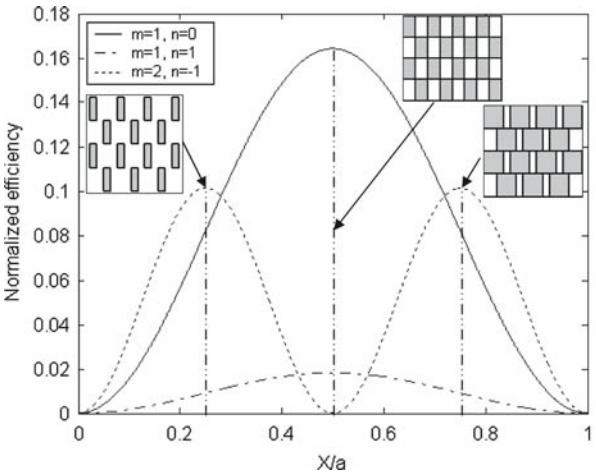

Fig. 5 Normalized efficiency of a hexagonal lattice with a rectangular motif $Y/a \sin 120° = 1$ as a function of the motif length to primitive vector magnitude ratio. Solid, dash-dotted, and dotted lines representing the efficiency curves for the (1, 0), (1, 1) and (2, −1) QPM orders, respectively. The three insets show the 2D NLPC for specific X/a ratios that maximize the efficiency for these orders

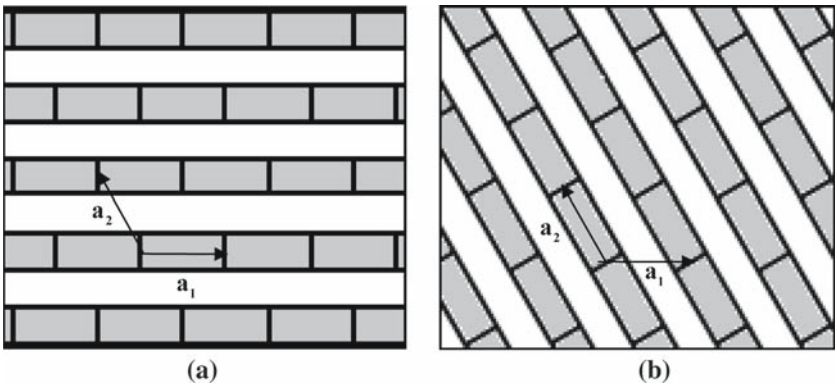

Fig. 6 A hexagonal lattice with a rectangular motif: (**a**) motif's edges parallel to $\mathbf{a_1}$, $X = |\mathbf{a_1}| = a$ (**b**) motif's edges parallel to $\mathbf{a_2}$, $Y = |\mathbf{a_2}| = a$

Table 3 Maximum of squared Fourier coefficient for rectangular lattice with rectangular motif

QPM order	Max of squared Fourier coefficient	$\frac{X}{a_1}$	$\frac{Y}{a_2}$
$m = 1, n = 0$	$\left\|G_{10}^{\max}\right\|^2 = 0.405$	0.5	1
$m = 1, \quad n = 1$	$\left\|G_{11}^{\max}\right\|^2 = 0.041$	0.5	0.5

of $|G_{01}|^2 = 0.405 = (2/\pi)^2$. This is the same optimal efficiency (for phase matching a single process) as that of a one-dimensional structure (Fejer et al. 1992). We note that with a different choice of rectangular motif, having edges parallel to $\mathbf{a_2}$, rather than to $\mathbf{a_1}$, one can get the same convergence into a one-dimensional periodic structure and the same efficiency for the (1, 0) order, as shown in Fig. 6b.

In the cases of rectangular and square lattices, the efficiency is also given by a multiplication of two sinc functions, as can be seen in Table 2b. This enables to optimize separately the X and Y values of the rectangular motif. Table 3 shows the maximum values of the squared Fourier coefficient for $(m, n) = (1, 0)$ and $(m, n) = (1, 1)$ for rectangular lattice.

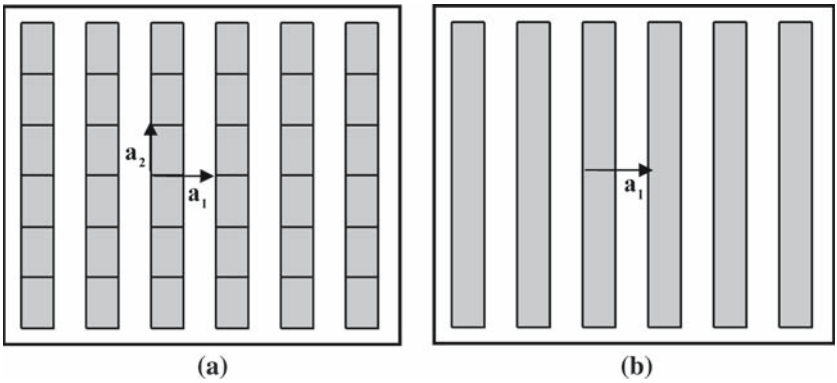

Fig. 7 (**a**) 2D rectangular lattice with $Y/a_2 = 1$ (**b**) 1D lattice

In the case of a rectangular lattice and for the $(1, 0)$ order, the optimum is obtained when $X/a_1 = 0.5$, $Y/a_2 = 1$. Note that this means that the rectangles along the $\mathbf{a_2}$ direction merge into a continuous line, as shown in Fig. 7. Hence, the two-dimensional structure becomes identical to a one-dimensional structure, in a similar fashion to the previously discussed $(0, 1)$ QPM order in a hexagonal lattice. Furthermore, it is easy to show that for an $(m, 0)$ order, the Fourier coefficient of a rectangular lattice, with coinciding rectangles in the Y direction, i.e., $Y/a_2 = 1$ is given by

$$G_{m0} = \frac{2}{m\pi} \sin\left(m\pi \frac{X}{a_1}\right) \tag{30}$$

which is exactly the Fourier coefficient of a 1D structure with a duty cycle of X/a_1 for an mth order QPM process (Fejer et al. 1992).

In fact, for all the five Bravais lattices, if we rely on a single reciprocal lattice vector, the optimal motif is a rectangular motif, and with suitable orientation of this motif, it converges into a one-dimensional periodic structure. Usually, a two-dimensional periodic structure is needed when more than one reciprocal lattice vector is required. Our analysis shows that there can be a continuous transition from a two-dimensional to a one-dimensional periodic structure. In addition, the values of the one-dimensional structure set the maximum limit on the conversion efficiency for the two-dimensional structure.

4 Discussion and summary

In this paper, we have presented a general analysis of quasi-phase-matched conversion efficiency in all possible periodic two-dimensional structures. This analysis enables to design and analyze structures for two-dimensional quasi-phase-matched frequency conversion, in any given periodic lattice and in any chosen QPM order.

We have shown that the conversion efficiency for optical intensities of a QPM process of some (m, n) order scales as $|G_{mn}|^2$. The value of the Fourier coefficient G_{mn} depends both on the choice of the periodic lattice and on the shape and dimensions of the nonlinear motif. A general expression that includes the effects of lattice, motif, and QPM order was derived in Eq. 16. The conversion efficiency is also determined by the interaction area, defined by the 2D NLPC area and beam parameters. We have analyzed two specific motifs, a circular motif

that may be realized in materials that are nearly isotropic in the X–Y plane, and a rectangular motif that can be used in highly anisotropic materials. The values of G_{mn} for all five possible periodic lattice structures and for the two choices of motifs are given in Table 2a and b.

Some specific examples of conversion efficiency were considered for two QPM orders, namely $(m, n) = (1, 0)$ and $(m, n) = (1, 1)$, for the cases of hexagonal, square, and rectangular lattices. We have found that for one single order that relies on a single reciprocal lattice vector, like $(1, 0)$ or $(m, 0)$, the highest efficiency is obtained with a rectangular motif. In fact, the optimal condition for phase matching a single process is such that the rectangular motifs of adjacent lattice point merge into a continuous line, and the structure becomes identical to a 1D QPM structure. If a circular motif is used, the rectangular lattice is the best choice in terms of efficiency for the $(1, 0)$ order, and the optimal condition is such that the circular motifs of adjacent lattice point just touch one another.

An interesting, and somewhat surprising result is that some specific choices of (m, n) QPM orders can provide significantly higher conversion efficiency than that of neighboring QPM orders. This can happen in hexagonal, centered-rectangular, and oblique lattices. For example, we have shown that the maximum efficiency of the $(2, -1)$ order in a hexagonal lattice with rectangular motif is five times more efficient than that of the $(1, 1)$ order.

Acknowledgements This work was partly supported by the Israel Science Foundation, grant no. 960/05.

References

Berger, V.: Nonlinear photonic crystals. Phys. Rev. Lett. **81**, 4136–4139 (1998)

Bratfalean, R.T., Peacock, A.C., Broderick, N.G.R., Gallo, K., Lewen, R.: Harmonic generation in a twodimensional nonlinear quasi-crystal. Opt. Lett. **30**, 424–426 (2005)

Broderick, N.G.R., Ross, G.W., Offerhaus, H.L., Richardson, D.J., Hanna, D.C.: Hexagonally poled lithium niobate: a two-dimensional nonlinear photonic crystal. Phys. Rev. Lett. **84**, 4345–4348 (2000)

Broderick, N.G.R., Bratfalean, R.T., Monro, T.M., Richardson, D.J., de Sterke, C.M.: Temperature and wavelength tuning of second-, third-, and fourth-harmonic generation in a two-dimensional hexagonally poled nonlinear crystal. J. Opt. Soc. Am. B **19**, 2263–2272 (2002)

Chowdhury, A., Staus, C., Boland, B.F., Kuech, T.F., McCaughan, L.: Experimental demonstration of 1535–1555-nm simultaneous optical wavelength interchange with a nonlinear photonic crystal. Opt. Lett. **26**, 1353–1355 (2001)

Fejer, M.M., Magel, G.A., Jundt, D.H., Byer, R.L.: Quasi-phase-matched second harmonic generation - tuning and tolerances. IEEE J. Quant. Electron. **28**, 2631–2654 (1992)

Giacovazzo, C., Monaco, H.L., Artioli, G., Viterbo, D., Ferraris, G., Gilli, G., Zanotti, G., Catti, M.: Fundamentals of crystallography. 2nd edn., University Press, Oxford (2002)

Glickman, Y., Winebrand, E., Arie, A., Rosenman, G.: Electron-beam-induced domain poling in LiNb03 for twodimensional nonlinear frequency conversion. Appl. Phys. Lett. **88**, 011103 (2006)

Jankovic, L., Kim, H., Stegeman, G., Carrasco, S., Torner, L., Katz, M.: Quadratic soliton self-reflection at a quadratically nonlinear interface. Opt. Lett. **28**, 2103–2105 (2003)

Kittel, C.: Introduction to solid state physics. 7th edn., Wiley, New York (1995)

Lifshitz, R., Arie, A., Bahabad, A.: Photonic quasicrystals for nonlinear optical frequency conversion. Phys. Rev. Lett. **95**, 133901 (2005)

Myers, R.A., Mukherjee, N., Brueck, S.R.J.: Large second-order nonlinearity in poled fused silica. Opt. Lett. **16**, 1732–1734 (1991)

Norton, A.H., de Sterke, C.M.: Optimal poling of nonlinear photonic crystals for frequency conversion. Opt. Lett. **28**, 188–190 (2003)

Ni, P., Ma, B., Wang, X., Cheng, B., Zhang, D.: Second-harmonic generation in two-dimensional periodically poled lithium niobate using second-order quasiphase matching. Appl. Phys. Lett. **82**, 4230–4232 (2003)

Peng, L.H., Hsu, C.C., Shih, Y.C.: Second-harmonic green generation from two-dimensional $\chi^{(2)}$ nonlinear photonic crystal with orthorhombic lattice structure. Appl. Phys. Lett. **83**, 3447–3449 (2003)

Russel, S.M., Powers, P.E., Missey, M.J., Schepler, K.L.: Broadband mid-infrared generation with twodimensional quasi- phase-matched structures. IEEE J. Quant. Electron. **37**, 877–887 (2001)

Saltiel, S., Kivshar, Y.S.: Phase matching in nonlinear $\chi^{(2)}$ photonic crystals. Opt. Lett. **25**, 1204–1206 (2000)
Saltiel, S.M., Kivshar, Y.S.: All-optical deflection and splitting by second-order cascading. Opt. Lett. **27**, 921–923 (2002)
Wang, X.H., Gu, B.Y.: Nonlinear frequency conversion in 2D $\chi^{(2)}$ photonic crystals and novel nonlinear doublecircle construction. Eur. Phys. J. B. **24**, 323–326 (2001)